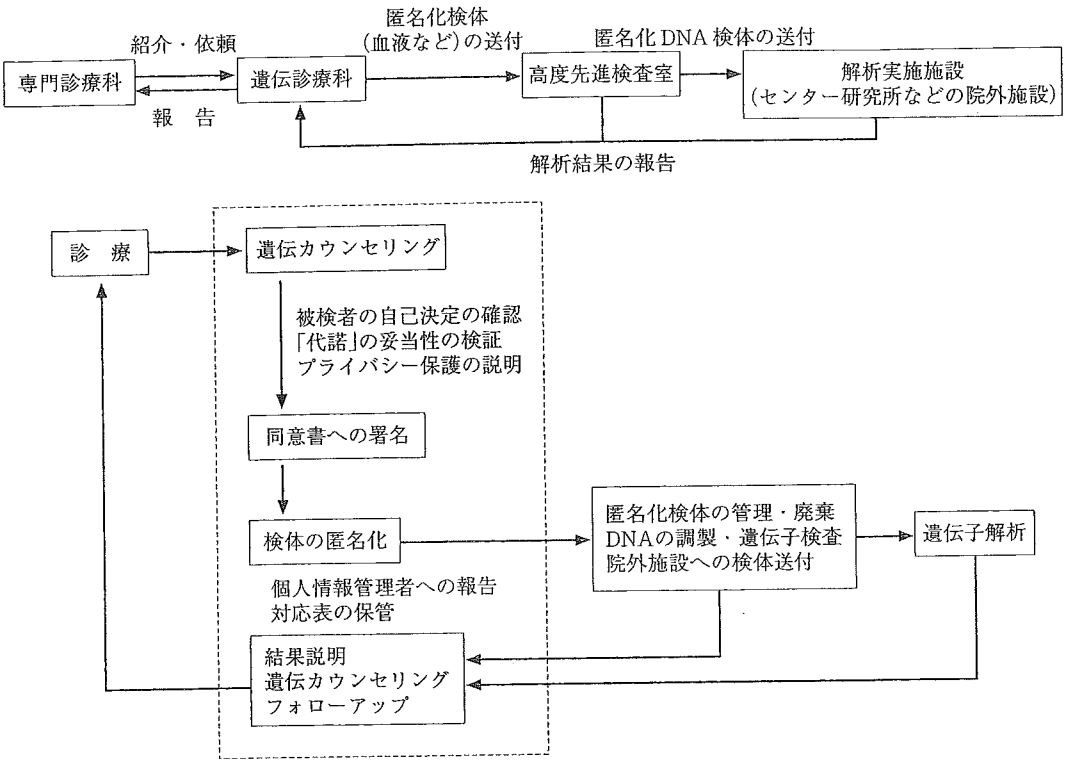

図1 国立成育医療センターにおける遺伝子検査のフロー

表2の実施要領を具体化したもの．国立成育医療センターでは遺伝子検査を行う際に全例で遺伝診療科スタッフ(臨床遺伝専門医)による事前のカウンセリングを必要とする．また，遺伝子検査を行う検体はすべて匿名化される．

2) GeneTests http://www.genetests.org/
3) いでんネット http://www.kuhp.kyoto-u.ac.jp/idennet/
4) Genetopia http://genetopia.md.shinshu-u.ac.jp/genetopia/index.htm

Early-Onset Macular Degeneration with Drusen in a Cynomolgus Monkey (*Macaca fascicularis*) Pedigree: Exclusion of 13 Candidate Genes and Loci

Shinsuke Umeda,[1,2] *Radha Ayyagari,*[3] *Rando Allikmets,*[4] *Michihiro T. Suzuki,*[5] *Athancios J. Karoukis,*[3] *Rajesh Ambasudhan,*[3] *Jana Zernant,*[4] *Haru Okamoto,*[1] *Fumiko Ono,*[5] *Keiji Terao,*[6] *Atsushi Mizota,*[7] *Yasuhiro Yoshikawa,*[2] *Yasuhiko Tanaka,*[1] *and Takeshi Iwata*[1]

Purpose. To describe hereditary macular degeneration observed in the cynomolgus monkey (*Macaca fascicularis*), which shares phenotypic features with age-related macular degeneration in humans, and to test the involvement of candidate gene loci by mutation screening and linkage analysis.

Methods. Ophthalmic examinations with fundus photography, fluorescein angiography (FA), indocyanine green angiography (IA), electroretinography (ERG), and histologic studies were performed on both affected and unaffected monkeys in the pedigree. The monkey orthologues of the human *ABCA4*, *VMD2*, *EFEMP1*, *TIMP3*, and *ELOVL4* genes were cloned and screened for mutations by single-strand conformation polymorphism (SSCP) analysis or denaturing high-performance liquid chromatography (DHPLC) and direct sequencing in six affected and five unaffected monkeys from the pedigree and in six unrelated, unaffected monkeys. Subsequently, 13 human macular degeneration loci including these five genes were analyzed to test for linkage with the disease. Nineteen affected and seven unaffected monkeys in the pedigree were analyzed by using human microsatellite markers linked to the 13 loci.

Results. Yellowish white spots were observed in the macula and fovea centralis, and in some cases the spots scattered to the peripheral retina along the blood vessels. FA showed hyperfluorescence corresponding to the dots except in the foveola. No anomalies were found by IA and ERG. Histologic studies demonstrated that the spots were drusen. Mutation analysis of the *ABCA4*, *VMD2*, *EFEMP1*, *TIMP3*, and *ELOVL4* genes identified a few sequence variants, but none of them segregated with the disease. Linkage analysis with markers linked to these five genes and an additional eight human macular degeneration loci failed to establish linkage. Haplotype analysis excluded the involvement of the 13 candidate loci for harboring the gene associated with macular degeneration in the monkeys.

Conclusions. Significant homology was identified between monkey and human orthologues of the five macular degeneration genes. Thirteen loci associated with macular degeneration in humans or harboring macular degeneration genes were excluded as causal of early-onset macular degeneration in the monkeys. It is likely that none of these loci, but rather a novel gene, is involved in causing the observed phenotype in this monkey pedigree. (*Invest Ophthalmol Vis Sci.* 2005;46:683-691) DOI:10.1167/iovs.04-1031

From the [1]National Institute of Sensory Organs, National Hospital Organization Tokyo Medical Center, Tokyo, Japan; the [2]Department of Biomedical Science, Graduate School of Agricultural and Life Sciences, The University of Tokyo, Tokyo, Japan; the [3]Department of Ophthalmology, Kellogg Eye Center, University of Michigan, Ann Arbor, Michigan; the [4]Departments of Ophthalmology and Pathology, Columbia University, New York, New York; The [5]Corporation for Production and Research of Laboratory Primates, Ibaraki, Japan; the [6]Tsukuba Primate Center for Medical Science, National Institute of Infectious Diseases, Ibaraki, Japan; and the [7]Department of Ophthalmology, Juntendo University Urayasu Hospital, Chiba, Japan.

Supported by research grant, Research on Measures for Intractable Diseases, Ministry of Health, Labor and Welfare of Japan and by the fellowship of the Promotion of Science for Japanese Junior Scientists (SU); The Foundation Fighting Blindness (RAI, RAy), National Eye Institute Grants EY13435 (RAI) and EY13198 (RAy), Research to Prevent Blindness (RAI, RAy) and Core Grant EY07003.

Submitted for publication August 27, 2004; revised November 1, 2004; accepted November 5, 2004.

Disclosure: **S. Umeda**, None; **R. Ayyagari**, None; **R. Allikmets**, None; **M.T. Suzuki**, None; **A.J. Karoukis**, None; **R. Ambasudhan**, None; **J. Zernant**, None; **H. Okamoto**, None; **F. Ono**, None; **K. Terao**, None; **A. Mizota**, None; **Y. Yoshikawa**, None; **Y. Tanaka**, None; **T. Iwata**, None

The publication costs of this article were defrayed in part by page charge payment. This article must therefore be marked "*advertisement*" in accordance with 18 U.S.C. §1734 solely to indicate this fact.

Corresponding author: Takeshi Iwata, National Institute of Sensory Organs, National Hospital Organization Tokyo Medical Center, 2-5-1 Higashigaoka, Meguro-ku, Tokyo 152-8902 Japan; iwatatakeshi@kankakuki.go.jp.

Investigative Ophthalmology & Visual Science, February 2005, Vol. 46, No. 2

The inherited macular dystrophies comprise a heterogeneous group of blinding disorders characterized by central visual loss and atrophy of the macula and underlying retinal pigment epithelium (RPE).[1] The complexity of the molecular basis of monogenic macular disease is being elucidated through identification of many of the disease-causing genes.[2-8] Because of limitations associated with studies in humans, nonhuman species with phenotypes similar to human macular degeneration have been used as model systems to study these diseases. Rodent models generated by altering the genes homologous to the disease-causing genes in humans are most extensively used in such studies; however, rodents do not have a defined macula and, hence, the clinical symptoms observed in humans with macular degeneration cannot be fully replicated.[9-11] Because the macula is found only in primates and birds, a monkey model of macular degeneration would be extremely valuable for studies elucidating the mechanism and etiology underlying these diseases. A primate model for macular degeneration is much needed to develop sensitive diagnostic techniques and potential therapeutic strategies to cure or prevent the disease. Furthermore, such models are of particular value if their genetic basis is understood.

Macular degeneration in monkeys was first described by Stafford in 1974.[12] He reported that 31 (6.6%) of eyes of elderly monkeys showed pigmentary disorders and/or drusen-like spots. In 1978, El-Mofty et al.[13] reported a high incidence (50%) of maculopathy in a closed rhesus monkey colony at the

Caribbean Primate Research Center of the University of Puerto Rico. The latest report from the center states that specific maternal lineages have a statistically significant higher prevalence of drusen.[14] Although they suspected the involvement of hereditary factors, genetic analysis of the macaque population has not been reported.

We have reported a high incidence of macular degeneration in one of the cynomolgus monkey (*Macaca fascicularis*) colonies at the Tsukuba Primate Center.[15,16] This macular degeneration originated from one affected male monkey, which showed phenotypic characterization of macular degeneration. The disease affects the central retina specifically, with yellowish white dots in the macula and lipofuscin deposits in the RPE, consistent with the phenotype observed in the early stages of age-related macular degeneration (AMD). These symptoms appear at the age of ~2 years and progress slowly throughout life. Mating experiments have demonstrated that this familial macular degeneration is segregating as an autosomal dominant trait.[17]

AMD is currently considered a multifactorial disorder involving both environmental and genetic factors. Recent studies have substantiated the evidence for AMD as a complex genetic disorder in which one or more genes contribute to an individual's susceptibility to the development of the disease.[18–20] To date, full-genome scan studies have indicated that some regions of the genome harbor AMD-predisposing genes.[21,22] However, most genes associated with susceptibility to AMD have not been identified, presumably because of a complex pattern of inheritance, late age of onset, and difficulties in obtaining large pedigrees for standard linkage analysis. Genes implicated in monogenic macular dystrophies that occur earlier in life with a clear pattern of inheritance have been considered as good candidates for susceptibility to AMD.[23–26] To date, 15 macular degeneration genes have been linked or cloned for human macular degeneration (RetNet; http://www.sph.uth.tmc.edu/Retnet/home.htm; provided in the public domain by University of Texas Houston Health Science Center, Houston, TX). However, with the exception of *ABCA4*, none of these genes has shown a convincing association with AMD.

Because the monkey macular degeneration model we present here shares phenotypic similarities with the early stages of AMD, the identification of the gene involved in this monkey pedigree may provide critical clues to the understanding of the mechanism of AMD. In this study, monkey orthologues of the human genes responsible for Stargardt macular degeneration 1 (*ABCA4*),[2] Best macular degeneration (*VMD2*),[3,7] Doyn honeycomb dystrophy (*EFEMP1*),[4] Sorsby fundus dystrophy (*TIMP3*),[5] and Stargardt macular degeneration 3 (*ELOVL4*)[6,8] were cloned and screened for mutations in the affected monkeys. Subsequently, 13 human macular degeneration loci, including these five genes, were analyzed to test for linkage with the disease in the pedigree. During this process, we evaluated the nature and utility of human microsatellite markers in the cynomolgus monkey for linkage studies. This article also describes the gene structure and evolutionary conservation of the five human macular degeneration genes in the cynomolgus monkey.

Materials and Methods

Maintenance of Monkeys

The cynomolgus monkeys in the pedigree with macular degeneration were reared at the Tsukuba Primate Center for Medical Science (National Institute of Infectious Diseases; Tokyo, Japan). All monkeys were treated in accordance with the rules for care and management of animals at the Tsukuba Primate Center[27] under the Guiding Principles for Animal Experiments using Non-Human Primates formulated and enforced by the Primate Society of Japan (1986). All experimental procedures were approved by the Animal Welfare and Animal Care Committee of the National Institute of Infectious Diseases of Japan. These animal protocols fulfill the guidelines in the ARVO Statement for the Use of Animals in Ophthalmic and Vision Research.

Clinical Studies

Fundus photographs, fluorescein angiography (FA), and indocyanine green angiography (IA) were performed with a fundus camera (TRC50; Topcon, Tokyo, Japan) in animals under anesthesia. Electroretinography (ERG) was recorded in four affected and six normal monkeys with a white/color LED stimulator and contact lens electrode (LS-W; Mayo, Aichi, Japan). After 20 minutes of dark adaptation, rod ERG, combined ERG, and oscillatory responses were recorded, and single-flash cone response and 30-Hz flicker ERG were recorded after 10 minutes of light adaptation. The stimulus and recording conditions conformed to the standards for clinical electroretinography recommended by the International Society for Clinical Electrophysiology of Vision.[28]

Genomic DNA and RNA Isolation

Peripheral blood was collected from 19 affected and 11 unaffected monkeys from the pedigree (Fig. 1, asterisks, pound signs) and an

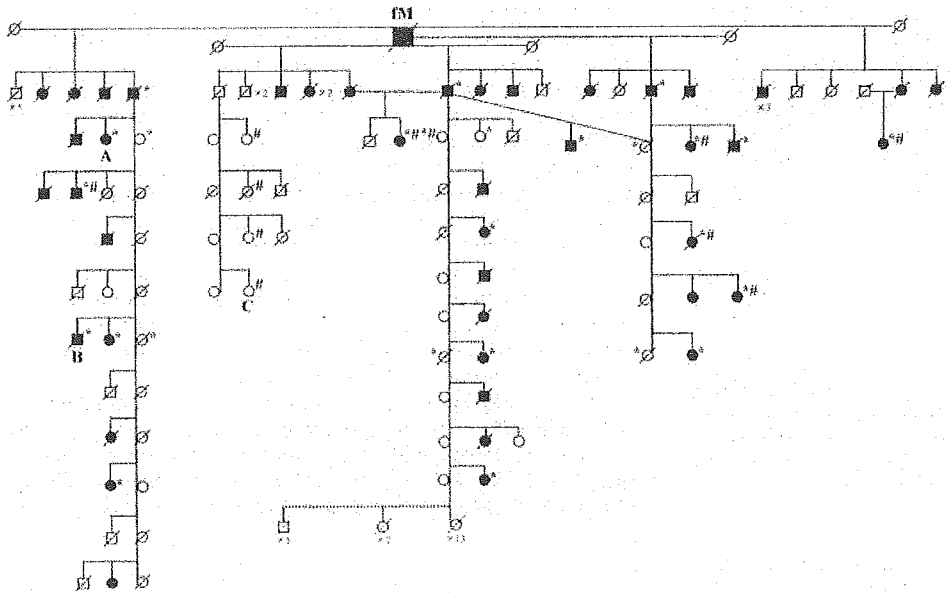

FIGURE 1. Edited version of the monkey pedigree with macular degeneration: fM, the founder breeding male monkey with typical macular degeneration, is shown with five healthy mates arrayed horizontally. The first-generation offspring are also arrayed horizontally. The breeding members from each branch of the first generation offspring are arrayed vertically with their mates and progeny. Monkeys used for *linkage analysis and #mutation screening are marked.

TABLE 1. Primer Sets Used for Cloning of the Monkey Homologues

Gene	Amplified Region	Name	Forward Primer	Position	Name	Reverse Primer	Position	Size (kb)
VMD2	Exon 1	P1F	GACCAGAAACCAGGACTGTTGA	Intron	P1R	GAACTCGCCATATAGCAGCTT	Exon 2	2.1
	Exon 2	P2F	GCTCTGACCAGGGTCTCTGA	Intron	P3R	CCGCACCTTTCCCTGAACTA	Intron	4.5
	Exon 3	P3F	CTAGACCTGGGGACAGTCTCA	Intron	P3R	CCGCACCTTTCCCTGAACTA	Intron	0.3
	Exon 4–5	P4F	CACGGAAGAACAACAGCTGA	Exon 3	P5R	ACACCAGTGGGATACTAATCCAG	Exon 6	2.3
	Exon 6	P6F	GCCAGGAATGGACCATGAGTA	Intron	P6R	GAGCCACTTAGCCTCTAGGTGA	Intron	0.3
	Exon 7–8	P7F	CCTGGAGCATCCTGATTTCA	Intron	P8R	TGAGGCCTCCCTACAGAACA	Intron	2.3
	Exon 9	P9F	TGGCAGAGCAGCTCATCA	Exon 8	P9R	AGCTTCCAGGCCTTGTTG	Exon 10	3.0
	Exon 10	P10F	AAGGGAGAAGGCCAGGTGTT	Intron	P10R	TTTCCTGTAGTGCTTGGGTACTA	Intron	1.2
	Exon 11	P11F	TGCCCTCCTACTGCAACATT	Intron	P11R	ATGCAATGGAGTGTGCATTA	Intron	1.1
EFEMP1	Exon 1	P1F	TTCTAGAACCCTCTGGTCTCTGA	Intron	P1R	CCCTTTCTTAACAGCAAGCTAAC	Intron	0.9
	Exon 2	P2F	GATTGGAAGTTGAGTATGGTGGA	Intron	P2R	CATTCTAGGGATAATGTGGTACCAA	Intron	1.3
	Exon 3–4	P3F	AAGATGGTACTGGGCAACTGTAC	Intron	P4R	ACATCTGTAGAGTAGCTTGACAGCA	Intron	1.4
	Exon 5	P5F	CTACACAGGCTAGAGGAATATGATCA	Intron	P5R	GACACAGGATTTAAGTAACTTGCTCA	Intron	1.3
	Exon 6–7	P6F	CACTGAATGGCATGAACATTG	Intron	P7R	TAGAACAGAATTCCCATGGGTAA	Intron	1.6
	Exon 8	P8F	AATAGGACAAGAAGCCAGATCTCT	Intron	P8R	TTCCTGGTTAAAACTAAATACCTAACA	Intron	0.4
	Exon 9–10	P9F	AACAGATGAACAATAGGTGCTTGA	Intron	P10R	TATCTATCTGGCAGTGTTACCAAGA	Intron	0.9
	Exon 11	P11F	GTATTAGACAAGGGATAAGAGCCAA	Intron	P11R	CAGAGGTTATGCATATATGCTGTGA	Intron	1.7
TIMP3	Exon 1	P1F	CCCAGCGCTATATCACTCG	Intron	P1R	AGCCACTGTGAGTTTCCTCTG	Intron	0.7
	Exon 2	P2F	CAATGGCTCTAACAGGAGAAGTAG	Intron	P2R	CTTGACCAAGGTCTCATGGTTA	Intron	0.8
	Exon 3–4	P3F	TCCAGTTCCAGCTGCATTG	Intron	P4R	AGTTAGTGTCCAAGGGAAGCT	Exon 5	2.6
	Exon 5	P5F	ATGTACCGAGGCTTCACCAA	Exon 3	P5R	AGGTGAGCTAAACACTATTCTGGA	Intron	3.5

additional six unrelated normal monkeys, and genomic DNA was extracted (QIAamp DNA Blood Maxi Kit; Qiagen, Valencia, CA). A normal monkey outside the pedigree was killed for bilateral eye enucleation, and enucleated eyes were immersed and stored in RNA-stabilization solution (RNAlater; Ambion, Austin, TX) at −80°C until RNA isolation. After thawing on ice, the eyeballs were dissected to separate the neural retina and choroid followed by extraction of total RNA.

Histologic Studies

An affected 14-year-old male monkey (Fig. 1, monkey B) was killed for histologic studies. Enucleated eyes were fixed in 10% neutralized formaldehyde solution at 4°C overnight, dehydrated, and embedded in paraffin. Four-micrometer-thick sections were prepared and stained with hematoxylin and eosin (HE) or periodic acid–Schiff (PAS). Serial sections were used for immunohistochemical analysis with anti-complement 5 (C5) antibody. After pretreatment with 0.4 mg/mL proteinase K in phosphate-buffered saline (PBS) for 5 minutes and blocking with 5% skim milk in PBS for 20 minutes at room temperature, the sections were incubated with rabbit anti-human C5 polyclonal antibody (Dako, Glostrup, Denmark) diluted to 1:200 dilution in PBS for 2 hours at room temperature. Alexa 488–conjugated goat anti-rabbit IgG (Molecular Probes, Eugene, OR), diluted to 1:200 in PBS, was used as the secondary antibody. The negative control experiments were performed using normal rabbit immunoglobulin fraction (Dako) instead of anti-C5 antibody.

Characterization of the Genomic Organization and cDNA Sequence of the Monkey *ABCA4*, *VMD2*, *EFEMP1*, and *TIMP3* Genes

Gene-specific primers of the human macular degeneration genes *ABCA4*, *VMD2*, *EFEMP1*, and *TIMP3* were designed based on the human genomic DNA sequence to amplify exons of monkey genes (Table 1). Amplified products were directly sequenced. For all genes except *ABCA4*, the 5′/3′-rapid amplification of cDNA ends (5′/3′-RACE) was performed using total RNA isolated from the monkey retina. Amplification of partial cDNAs by both 5′- and 3′-RACE was designed to generate overlapping PCR products to obtain a full-length cDNA sequence. Primers were initially designed based on the exonic sequences obtained by genomic sequence (Table 2). RACE products were subcloned into the pCRII cloning vector (TA Cloning Kit Dual Promoter; Invitrogen, Carlsbad, CA) and sequenced directly. The obtained nucleotide sequence data have been submitted to GenBank, and assigned accession numbers: *TIMP3*: AY207381–207385, AH012631; *EFEMP1*: AY312407–312415, AH012997; *VMD2*: AY357925–357936, AH013172; *ELOVL4*: AF461182–461187, AH012403; *ABCA4*; AY793687 (http://www.ncbi.nlm.nih.gov/Genbank; provided in the public domain by the National Center for Biotechnology Information, Bethesda, MD).

Mutation Analysis

Coding regions and adjacent intronic sequences of the monkey *ABCA4*, *VMD2*, *EFEMP1*, *TIMP3*, and *ELOVL4* genes were analyzed for sequence variants by single-strand conformation polymorphism (SSCP) or denaturing (D)HPLC (for the *ABCA4* gene) analysis in parallel with direct sequencing. Genomic DNA from six affected and five unaffected monkeys from the pedigree (Fig. 1, pound signs) and six unrelated normal subjects were used for mutation analysis. Primers located in the intronic regions were designed to amplify coding sequences of individual genes (Table 3). Large exons were divided into smaller segments to obtain amplification products suitable for SSCP analysis. The purified amplicons were analyzed by SSCP or DHPLC analysis, as previously described.[29,30] All the samples were also analyzed by bidirectional sequencing with the PCR primers. Exons 2, 7, and 10 of the *VMD2* gene were screened for sequence variants only by direct sequencing.

TABLE 2. Primers for 5′–3′-RACE

Gene	5′-RACE	Position	3′-RACE	Position
VMD2	GTATACACCAGTGGGATA	Exon 6	AGAGCAACAGCTGATGTTTGAGAA	Exon 3
EFEMP1	GGATGGTACATTCATCTA	Exon 7	GATCCTGTGAGACAGCAATGCA	Exon 3
TIMP3	ATCATCTGGGAAGAGTTA	Exon 5	GATGAAGATGTACCGAGGCTTCA	Exon 2–3

TABLE 3. Primer Sets Used for Mutation Screening

Gene	Exon No.	Length (bp)	Name	Forward Primer	Name	Reverse Primer	Size (bp)
ABCA4	1	66	01F	TCTTCGTGTGGTCATTAGC	01R	ACCCCACACTTCCAACCTG	152
	2	94	02F	AAGTCCTACTGCACACATGG	02R	CTAGACAAAAGGCCCAGACC	266
	3	142	03F	TTCCCAAAAAGGCCAACTC	03R	CACGCACGTGTGCATTTCAG	301
	4	139	04F	GCTATTTCCTTATTAATGAGGC	04R	GGGAAATGATGCTTGAGAGC	212
	5	128	05F	CCCTTCAACACCCTGTTCTT	05R	TTCTTGCCTTTCTCAGGCTGG	237
	6	198	06F	GTATTCCCAGGTTCTGTGG	06R	TACCCCAGGAATCACCTTG	330
	7	88	07F	AGCATATAGGAGATCAGACTG	07R	GGCATAAGAGGGGTAAATGG	241
	8	238	08F	GAGCATTGGCCTCACAGCAG	08R	CCCCAGGTTTGGTTTCACC	397
	9	139	09F	AGACATGTGATGTGGATACAC	09R	GTGGGAGGTCCAGGGTACAC	271
	10	117	10F	AACACTAAGTGATAGGGGCAGAA	10R	GGCCTGCTTGTTGTATTTTGAT	344
	11	198	11F	AGCTCACTCGCTCTTTAGGG	11R	TTCAAGACCACTTGACTTGC	406
	12	206	12F	TGGGACAGCAGCCCTTATC	12R	CCAAATGTAATTTCCCACTGAC	362
	13	177	13F	AATGAGTTCCGAGTCACCCTG	13R	CCCATTAGCGTGTCATGG	308
	14	223	14F	TCCATCTGGGCTTTGTTCTC	14R	AATCCAGGCACATGAACAGG	407
	15	222	15F	AGACAGTAACTAACAGGCTCGTG	15R	GGACTGCTACAGACCCTTCC	386
	16	205	16F	CTGTTGCATTGGATAAAAGGC	16R	GATGAATGGAGAGGGCTGG	330
	17	65	17F	CTGCGGTAAGGTAGGATAGGG	17R	CACACCGTTTACATAGAGGGC	232
	18	90	18F	CAGCTCCCGGTGGTAGAGTA	18R	CCCTTGCCATGAGATGTTTT	222
	19	175	19F	TGGGGCCATGTAATTAGGC	19R	TGGGAAAGAGTAGACAGCCG	322
	20	132	20F	GCATGTTGCTAAAGGCCATC	20R	TATCTCTGCCTGTGCCCAG	293
	21	140	21F	GTAAGATCAGCTGCTGGAAG	21R	GAAGCTCTCCTGCTCCAAGC	301
	22	138	22F	CCCTCCACAGTCCCTTAACTC	22R	GAGAGTGGGGACCACAGGTA	244
	23	194	23F	TTTTGCAACTATGTAGCCAGGA	23R	AGCCTGTGTGAGTAGCCATG	384
	24	85	24F	GCATCAGGGAGAGGCTGTC	24R	CCCAGCAATATTGGGAGATG	212
	25	206	IVS24F	GTAAGGACTGGACGGGCCATACTTGG	IVS24R	TCCAGCTCTCTGAAAAGGCTGGCATA	2 kb
			IVS25F	AAAGCTGGTGGAGTGCATTGGTCAAG	IVS25R	CCTGAATCAGAATCCTCCGTGACCTTC	500
	26	49	26F	TCCCATTATGAAGCAATACC	26R	ACCCAGCCCCTTAGACTTTC	228
	27	266	IVS26F	GGATTCTGATTCAGGACCTCTGTTTGC	IVS26R	CTGCGGATGGTGTGTTGGAATCTCTT	2 kb
			IVS27F	TCCCAGAGAGAAGGCTGGACAGACAC	IVS27R	CCCATATATCCAGGGGTGAAGGGTCA	1 kb
	28	125	28F	TGCACGCGCACGTGTGAC	28R	TGAAGGTCCCAGTGAAGTGGG	291
	29	99	29F	CAGCAGCTATCCAGTAAAGG	29R	AACGCCTGCCATCTTGAAC	263
	30	187	30F	GTTGGGCACAATTTCTTATGC	30R	ACTCAGGAGATACCAGGGAC	347
	31	95	IVS30F	GAGAAGCTCACCATGCTGCCAGAGT	IVS30R	GAGATGTTCCTGTCCGTCAGGTCTTG	2 kb
			IVS31F	CGCAGCACGGAAATTCTACAAGACCT	IVS31R	CCTCTGTTCATTGACCCAGAATTTGCT	700
	32	33	32F	ACGGCACTGCTGTACTTGTG	32R	TCAACATGGCTGTGAGGTGT	182
	33	106	IVS32F	GAGCAAATTCTGGGTCAATGAACAGAGG	IVS32R	CGCTTAAAAACCCAACAAGTGCTTCC	1.2 kb
			IVS33F	AGGTATGGAGGAATTTCCATTGGAGGA	IVS33R	CTTTAGAGGCCTCTCTAGTGATAGG	300
	34	75	34F	AAACCGTCTTGTTTGTTTGTTT	34R	AGGAGGGAGGGAATTCAATG	208
	35	170	IVS34F	GGCCCTATCACTAGAGAGGCCTCTAAAG	IVS34R	GGTTGGCTAATGACGGTGATTCCATAC	550
			IVS35F	CATGCCCTGGTCAGCTTTCTCAATGT	IVS35R	GAGAAAATCACGCAGATGGCAACCAC	2 kb
	36	178	36F	TGTAAGGCCTTCCCAAAGC	36R	TGGTCCTTCAGAGCACACAC	346
	37	116	37F	CATTTTGCAGAGCTGGCAGC	37R	CTTCTGTCAGGAGATGATCC	260
	38	158	38F	GGAGTGCATTATATCCAGACG	38R	CCTGGCTCTGCTTGACCAAC	302
	39	125	39F	TGCTGTCCTGTGAGAGCATC	39R	CTTCCAGCCCAACAAGGTC	344
	40	130	IVS39F	CTGCTCATTGTCTTCCCCCACTTCTG	IVS39R	CAGCAGGGTCAGGAGGAAGTACACCA	700
			IVS40F	GTGAGGAGCACTCTGCAAATCCGTTC	IVS40R	AGATGAGGAAAAGGGGTCAGGATTGG	3.5 kb
	41	121	41F	GAAGAGAGGTCCCATGGAAAGG	41R	GCTTGCATAAGCATATCAATTG	299
	42	63	42F	CTCCTAAACCATCCTTTGCTC	42R	AGGCAGGCACAAGAGCTG	214
	43	107	43F	GGTCTCTAGGGCCAGGCTA	43R	CACATCTTTCAGGGCCTCAG	271
	44	142	44F	GAAGCTTCTCCAGCCCTAGC	44R	TGCACTCTCATGAAACAGGC	277
	45	135	IVS44F	ACATCTTTACCTTTATGCCCGGCTTCG	IVS44R	AATGAGTGCGATGGCTGTGGAGAGTT	4 kb
			IVS45F	TTAAGAGCCTGGGCCTGACTGTCTACG	IVS45R	GAATCTCTTGCCTGTGGGATGTGAGG	1 kb
	46	104	48F	GAAGCAGTAATCAGAAGGGC	46R	GCCTCACATTCTTCCATGCTG	257
	47	93	47F	TCACATCCCACAGGCAAGAG	47R	TTCCAAGTGTCAATGGAGAAC	258
	48	250	48F	ATTACCTTAGGCCCAACCAC	48R	ACACTGGGTGTTCTGGACC	365
	49	87	49F	GGTGTAGGGTGGTGTTTTCC	49R	ACTGCCTCAAGCTGTGGACT	187
VMD2	2*	152	P2F	GCTCTGACCAGGGTCTCTGA	P3R	CCGCACCTTTCCCTGAACTA	4.5 kb
	3	95	P3F	CTAGACCTGGGGACAGTCTCA	P3R	CCGCACCTTTCCCTGAACTA	325
	4	234	MP4aF	TGGGAGACAGAACCCTTGGA	MP4aF	GTCCTTGCCTTCCACGAA	302
			MP4bF	TGGTGGAACCAGTACGAGAA	MP4bF	TCCACCCATCTTCCATTGTT	286
	5	155	MP5F	AAAGGAGTGCTGAGGTTCCTATA	MP5R	CTTGTTTCCTGTGAACCACAA	330
	6	78	P6F	GCCAGGAATGGACCATGAGTA	P6R	GAGCCACTTAGCCTCTAGGTGA	292
	7*	153	P7F	CCTGGAGCATCCTGATTTCA	P8R	TGAGGCCTCCCTACAGAACA	2.3 kb
	8	81	MP8F	GCATCATGTGGTGTGGAAAT	P8R	TGAGGCCTCCCTACAGAACA	270
	9	152	MP9F	CAAGTCATCAGGCACGTACAA	MP9R	CTAGGCAGACCCCTGCTACTA	286
	10*	639	P10F	AAGGGAGAAGGCCAGGTGTT	P10R	TTTCCTGTAGTGCTTGGGTACTA	1.2 kb
	11	19	P11F	TGCCCTCCTACTGCAACATT	MP11R	AAGTAGTCCTGGACTGCTGATTT	270
EFEMP1	2	81	MP2F	CCGCAGCAGATACTAAATATCAG	MP2R	CCGCTGAACCGTACTTATTTC	173
	3	49	MP3F	CTTAGGGAATGGACACACCAA	MP3R	ACAGAAGGCCAAAGATCACAT	155

(continues)

TABLE 3. (*continued*).

Gene	Exon No.	Length (bp)	Name	Forward Primer	Name	Reverse Primer	Size (bp)
	4	387	MP4aF	CCCTCTTAGAAGATTCCTGACTTA	MP4aR	ACACTCCACTGGTTGCCAT	249
			MP4bF	ATGAACAGCCTCAGCAGGA	MP4bR	GCAAAAGCTTTCGATGGTTA	316
	5	123	MP5F	GGAGGCAATATCAACATCTTCA	MP5R	TGCTTGAGGTTGAAACAGTTAAG	248
	6	120	MP6F	GCAAACAGCAATGCTAATTCA	MP6R	GAAATACTGCAACATGGCATG	250
	7	120	MP7F	CAGCTAGGGAATTATTTATCAGCA	MP7R	CAGGGATTGGACTTTATTCCA	279
	8	120	MP8F	ATATCCAAAGTAGTGGTGCACAA	P8R	TTCCTGGTTAAAACTAAATACCTAACA	235
	9	124	MP9F	TGCAAACAGAATCTGCCAGTA	MP9R	TTTGGCTTGGTAAGACCAGAA	265
	10	196	MP10F	CTTACCAAGCCAAACTGCTAACTA	MP10R	AACAAACTCCCATCTTTCTCAATAG	289
	11	162	MP11F	AAAGCATAGAAACTCCAATGCA	MP11R	AGGTAACAATATTCTTTGGCTGACT	281
ELOVL4	1	100	MP1F	CCGCGGTTAGAGGTGTTC	MP1R	GAGACCAGGGGTCGGTGAC	281
	2	188	MP2aF	TTGAGACATCTTGATTCCTAGAAAG	MP2aR	AAGTTAAGCAAAACCATCCCA	252
			MP2bF	CTGGGTCCAAAGTGGATGAA	MP2bR	AGCTAACAGTTATGTCTGGGTACAA	213
	3	81	MP3F	GCAATTGGAATGCATGACA	MP3R	TTTCACAGATTGGGGCCTATA	304
	4	172	MP4aF	AAATGATTCCATGCCTTGTACA	MP4aR	AACGCAAGCAGTATATTCCTGA	330
			MP4b	TGGTGTTTATAACAGGCTTTCC	MP4bR	CTCATTGCTTTCCACTGAACA	271
	5	128	MP5F	ATCTCGGTGGCTTACTGCTTA	MP5R	AATAAGTCGGCTGGAGTCAACT	356
	6	276	MP6aF	TTGGGCCTGTGATAGCTATG	MP6aR	TTAGGCTCTTTGTATGTCCGAA	247
			MP6bF	CTCTAATTGCCTACGCAATCAG	MP6bR	GGGAGTTTTTCCTCACTGTCA	242
TIMP3	1	121	MP1F	AACTTTGGAGAGGCGAGCA	MP1R	CCTAAGCAGCGCTGCAGTC	233
	2	83	MP2F	TGAGATGCTGTTCCTGATGTG	MP2R	GGCTGGTGCTTAGACACACA	266
	3	112	MP3F	AGCAGTGGGATTATGGATCATAC	MP3R	ACATTTGGTGAGTCAGCTACTCA	267
	4	122	MP4F	TGGGCTAAGTGGGAACATAGTA	MP4R	GTTTCTAGGGCTGCAAGTCA	274
	5	198	MP5F	TACCATGGCAGATTCCATCA	MP5R	AGTTAGTGTCCGAGGGAAGCT	306

* Exon 2, 7, and 10 of the *VMD2* gene were screened for sequence variants only by direct sequencing.

Linkage Analysis

Linkage analysis was performed on DNA from 19 affected and 7 unaffected members of the pedigree. Individuals used for the analysis are indicated by asterisks in Figure 1. Human microsatellite markers linked to human macular degeneration loci were analyzed with monkey genomic DNA used as the template. Details of microsatellite markers and their primer sequences were obtained from the genome database. Microsatellite marker analysis was performed by two methods: Markers linked to candidate gene loci and included in a linkage mapping set (ver. 2.5MD10; Applied Biosystems, Inc. [ABI], Foster City, CA) were analyzed on the a DNA sequencer (model 3100; ABI) with fluorescence-labeled primers. Additional microsatellite markers were analyzed by ^{32}P dCTP incorporation into the amplified product.[31] Two-point linkage analysis was performed between the disease locus and microsatellite markers with the MLINK program of the LINKAGE package, as described elsewhere.[32,33] Linkage was assessed under the conditions of autosomal dominant inheritance of the disease trait with a frequency of 0.001 for the disease-causing allele, by using the affecteds-only model, as published earlier.[34] Linkage analysis was performed assuming equal frequencies for marker alleles. Haplotypes were constructed with genotypes of microsatellite markers according to their order on human chromosomes.

RESULTS

Clinical and Histologic Findings

Fundus photographs and FA of a 14-year-old female affected monkey (Fig. 1, monkey A) are shown in Figure 2. Fine, yellowish white dots were observed in the maculae (Figs. 2a–d), scattered in the peripheral retina along blood vessels in this monkey (Figs. 2a, 2b). However, in most cases, the locations of the lesions fell within the region centered on the fovea centralis with the same diameter as one optic disc. FA showed hyperfluorescence corresponding to these dots, except foveola (Figs. 2e, 2f). No abnormalities were found in the optic disc, retinal blood vessels, or choroidal vasculatures in any eyes examined. The amplitude and peak latency of both dark- and light-adapted ERG showed no alteration compared with normal control eyes, indicating that global rod or cone degeneration was absent. Histologic studies demonstrated that there were various-sized drusen, weakly stained by PAS (light purple), between the RPE and choriocapillaris in the macular region (Figs. 3a, 3b, asterisk). These drusen were strongly reactive with antibodies against complement C5 (Figs. 3c, 3d). This finding was consistent with the property of drusen reported in patients with AMD.[35] Accumulation of lipofuscin in RPE cells was also obvious by PAS (Figs. 3a, 3b, deep purple, arrows).

Mutation Analysis of the *ABCA4*, *VMD2*, *EFEMP1*, *TIMP3*, and *ELOVL4* Genes

To evaluate the involvement of the *ABCA4*, *VMD2*, *EFEMP1*, *TIMP3*, and *ELOVL4* genes in disease, we first determined the genomic sequence and the complete cDNA sequence of the orthologous genes in the monkey. Subsequently, these genes were screened for sequence variants in affected and unaffected monkeys in the pedigree, in addition to unrelated, unaffected animals by SSCP, or by DHPLC for the *ABCA4* gene, analysis and direct sequencing.

ABCA4. The monkey *ABCA4* gene consists of 50 exons, with its translation stop codon in exon 50, similar to the human gene. The complete 6819-bp cDNA encodes a protein of 2273 amino acids. *ABCA4* is a member of the superfamily of ATP-binding cassette (ABC) transporters, which are associated with membranes and transport various molecules across extra- and intracellular membranes of all cell types. ABC genes typically encode four domains that include two conserved ATP-binding domains and two domains with multiple transmembrane segments. Comparative sequence analysis revealed that the monkey ABCA4 protein was only 1.8% (41 amino acids) different from the human orthologue, whereas the sequence was identical in the two adenosine triphosphate (ATP)-binding domains. Five of the 41 nonconserved amino acids in the monkey protein (codons 223, 423, 1300, 1817, and 2255) involve polymorphisms in the human. Surprisingly, the Lys223Gln and Arg1300Gln changes reported to be associated with Stargardt disease in humans were observed in the homozygous state in

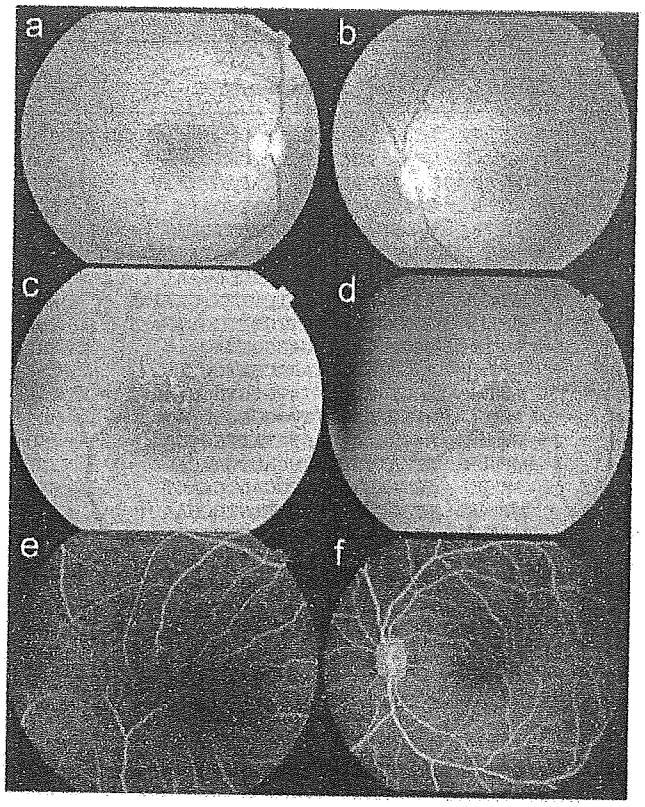

FIGURE 2. Fundus photographs and fluorescein angiogram (FA) of a 14-year-old female cynomolgus monkey (Fig. 1, monkey A) with macular degeneration, showing the right (**a**, **c**, **e**) and left (**b**, **d**, **f**) posterior poles. Fine *grayish white* or *yellowish white* dots were visible in the macula (**a**–**d**). The dots were observed in the peripheral retina along blood vessels in this monkey (**a**, **b**). These dots showed hyperfluorescence in FA except in the foveola (**e**, **f**). High-magnification of the macular region (**c**, **d**, **e**).

one normal control monkey (Fig. 1, monkey C). In addition, the mutation analysis revealed heterozygous amino acid changes at five positions—Leu424Val, Arg1017His, Val1114Ile, Ile1615Val, and Pro2238Gln—in both affected and normal monkeys. However, these missense variants did not segregate with the disease phenotype.

VMD2. The monkey *VMD2* gene consists of 11 exons, with its translation initiation codon in exon 2, as observed in its human orthologue. The complete cDNA was 2187 bp, encoding 585 amino acids. The *VMD2* gene encodes the bestrophin protein, which localizes to the basolateral plasma membrane of the RPE with the postulated function as an oligomeric chloride channel.[36,37] The hydropathy profile predicted that bestrophin contains four stretches of hydrophobic amino acids that function as transmembrane domains. Comparative sequence analysis demonstrated that monkey bestrophin had 19 amino acids different from its human homologue, and the four putative transmembrane domains are highly conserved. To date, 72 disease-associated nucleotide substitutions of the *VMD2* gene have been identified in patients with Best disease.[3,7,26] The mutation analysis of the *VMD2* gene in the monkey pedigree detected six amino acid sequence variants. A polymorphism (Val/Ile) was detected at codon 275 in the fourth transmembrane domain, which has also been reported in humans.[26] Four polymorphisms (Tyr465His, Thr542Met, Glu557Gln, and Thr566Ala) were detected in exon 10. These changes did not segregate with the disease. In addition, one nonsense mutation at codon 582 (Glu→Stop) in exon 11 was detected in two normal monkeys, whereas none of the examined six affected monkeys showed the change.

EFEMP1. The exon-intron gene structure of the monkey *EFEMP1* gene was also similar to the human *EFEMP1* gene. It was composed of 11 exons with its translation initiation codon in exon 2. The complete cDNA was 2034 bp, encoding 493 amino acids. Although the function of this gene remains unclear, this class of proteins is known to have characteristic sequence of repeated calcium-binding EGF-like domains.[4] The monkey *EFEMP1* cDNA was found to have six EGF repeats. Four EGF repeats (numbers 2–5) are encoded by single exons (exons 5–8), one EGF repeat (number 1) is encoded by three exons (exons 2–4), and EGF repeat number 6 is encoded by two exons (exons 9, 10). This finding is in agreement with one of the two transcriptional variants with a distinct 5′ untranslated region (UTR) described in its human homologue. Comparative sequence analysis demonstrated that the monkey *EFEMP1* has three amino acids different from that of the human, but the sequence in the entire region of six EGF repeats is completely conserved. In humans, a single mutation (Arg345Trp) that disrupts one of these domains is known to cause Malattia Leventinese.[4] No amino acid-changing polymorphisms were found in all the monkeys tested. Three single nucleotide polymorphisms (SNPs), that did not alter the amino acid sequence, were detected in exons 4, 5, and 10.

TIMP3. The monkey *TIMP3* gene consisted of five exons, similar to its human orthologue. The complete cDNA was 1887 bp in length, encoding 211 amino acids. *TIMP3* is the third member of the tissue inhibitors of metalloproteinase family, a group of zinc-binding endopeptidases involved in the degradation of the extracellular matrix. *TIMP3* has 12 cysteines characteristic of the TIMP family, which are proposed to form intramolecular disulfide bonds and tertiary structure for the functional properties of the mature protein. The predicted amino acid sequence of the monkey *TIMP3* gene was identical with the human orthologue, including the 12 cysteine residues. Mutations in the *TIMP3* gene are known to cause Sorsby's fundus dystrophy.[5] With a few exceptions,[38,39] most previously described mutations disrupt the disulfide bonds by changing residues into cysteines, leading to misfolding of the protein.[5,40] No coding sequence changes were detected in the *TIMP3* gene in monkeys by mutation screening.

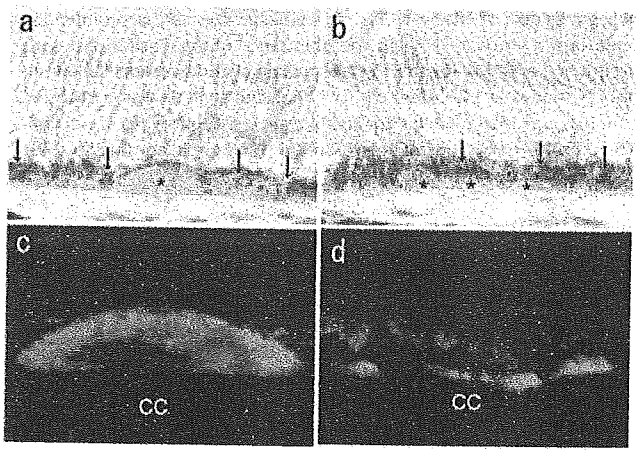

FIGURE 3. Drusen in the affected monkey retina. An affected 14-year-old male monkey (Fig. 1, monkey B). There were various-sized drusen, which were weakly stained by PAS (*), between the RPE and choriocapillaris (CC) (**a**, **b**). These drusen were strongly reactive with antibodies against complement C5 (*green* channel). Lipofuscin autofluorescence is shown (*red*) in the RPE (**c**, **d**). Accumulation of lipofuscin in RPE cells was also obvious by PAS (**a**, **b**, *arrows*).

TABLE 4. Two-Point Lod Scores between the Monkey Macular Degeneration Locus and Markers at the Human Macular Degeneration Loci

Markers	Distance from the Gene (CM)	Order on the Chromosome (M)	Lod Scores at θ									Exclusion ($Z = -2$)
			0	0.001	0.005	0.01	0.05	0.1	0.2	0.3	0.4	
CORD8		154.28										
D1S431	10.5	165	$-\varepsilon$	−2.116	−1.422	−1.128	−0.483	−0.248	−0.071	−0.01	0.006	0.001
D1S2635	0	154.28	$-\varepsilon$	−11.078	−7.598	−6.112	−2.773	−1.469	−0.392	0.019	0.119	0.075
D1S2715	−6.9	147.01	$-\varepsilon$	−7.7	−4.925	−3.747	−1.162	−0.232	0.388	0.464	0.299	0.03
D1S498	−10.6	144.94	$-\varepsilon$	−1.124	−0.439	−0.154	0.416	0.564	0.567	0.433	0.227	0.0001
ABCA4		94.1										
D1S188	−2.3	91.7	$-\varepsilon$	−6.139	−4.058	−3.175	−1.24	−0.541	−0.05	0.074	0.066	0.01
D1S2849	−1.2	92.9	$-\varepsilon$	−1.766	−1.075	−0.784	−0.166	0.032	0.133	0.119	0.067	
D1S2868	0.1	94	$-\varepsilon$	−14.824	−10.623	−8.809	−4.599	−2.846	−1.264	−0.522	−0.146	0.1
STGD3		80.5										
D6S1662	−2.67	77.83	$-\varepsilon$	−1.232	−0.544	−0.257	0.324	0.476	0.472	0.34	0.17	0.0
D6S1048	0.28	80.78	$-\varepsilon$	−0.063	0.614	0.889	1.38	1.416	1.172	0.79	0.362	0.0
D6S1596	7.1	87.6	$-\varepsilon$	−8.746	−5.965	−4.78	−2.138	−1.127	−0.319	−0.025	0.049	0.05
D6S1609	12.08	92.58	$-\varepsilon$	−7.326	−5.235	−4.34	−2.302	−1.475	−0.724	−0.349	0.131	0.05
DHRD		56.1										
D2S2230	3.9	60	$-\varepsilon$	−11.691	−8.209	−6.719	−3.349	−2.006	−0.842	−0.325	−0.084	0.1
D2S378	1.1	57.2	$-\varepsilon$	−9.268	−6.482	−5.29	−2.593	−1.517	−0.588	−0.186	−0.019	0.05
ARMD1		192.2										
D1S384	−2.11	190.09	$-\varepsilon$	−5.565	−3.486	−2.606	−0.696	−0.032	0.375	0.389	0.236	0.01
D1S413	2.1	194.1	$-\varepsilon$	−11.068	−7.59	−6.106	−2.784	−1.501	−0.46	−0.067	0.047	0.05
D1S2622	3.7	195.9	$-\varepsilon$	−1.961	−1.271	−0.982	−0.375	−0.185	−0.084	−0.066	−0.047	0.0
VMD2		61.5										
D11S1993	−2.3	59.2	$-\varepsilon$	−1.615	−0.925	−0.636	−0.032	0.151	0.224	0.181	0.1	0.0
D11S4174	1.4	62.9	$-\varepsilon$	−7.132	−5.026	−4.112	−1.979	−1.102	−0.368	−0.087	0.003	0.01
D11S4076	7.3	66.8	$-\varepsilon$	−5.617	−3.537	−2.656	−0.736	−0.061	0.364	0.385	0.231	0.01
Rhodopsin		130.6										
D3S3515	−4.01	126.59	$-\varepsilon$	−2.756	−1.379	−0.803	0.383	0.717	0.775	0.584	0.302	0.001
D3S3720	−2.8	127.8	$-\varepsilon$	−2.626	−1.247	−0.67	0.531	0.879	0.945	0.729	0.389	0.001
D3S1269	0.3	130.9	$-\varepsilon$	−11.566	−8.081	−6.588	−3.2	−1.846	−0.7	−0.238	−0.062	0.05
Timp3		31.5										
D22S1162	7.05	38.55	$-\varepsilon$	−3.587	−2.203	−1.619	−0.365	0.055	0.291	0.276	0.159	0.005
D22S280	0	31.5	$-\varepsilon$	−4.051	−2.664	−2.075	−0.785	−0.321	−0.002	0.065	0.044	0.01
D22S273	−1	30.5	$-\varepsilon$	−1.878	−1.187	−0.896	−0.278	−0.078	0.026	0.025	0.004	0.0
CTRP5		118.7										
D11S4127	−1.6	117.1	$-\varepsilon$	−0.771	−0.088	0.192	0.73	0.827	0.719	0.495	0.244	0.0
D11S924	0.2	118.9	$-\varepsilon$	−1.424	−0.736	−0.449	0.137	0.298	0.322	0.232	0.113	0.0
D11S4129	4.48	121.58	$-\varepsilon$	−9.057	−6.275	−5.089	−2.435	−1.41	−0.566	−0.214	−0.054	0.05
STGD4		26.1										
D4S403	0	26.1	$-\varepsilon$	−16.798	−11.919	−9.83	−5.081	−3.159	−1.445	−0.633	−0.206	0.1
D4S391	1.2	27.3	$-\varepsilon$	−3.615	−2.231	−1.647	−0.392	0.026	0.255	0.234	0.13	0.005
CORD5	(Interval)	64.5										
D17S938	0	64.5	$-\varepsilon$	−16.296	−11.422	−9.339	−4.638	−2.776	−1.176	−0.466	−0.125	0.1
D17S796	0	64.5	$-\varepsilon$	−3.594	−2.209	−1.624	−0.358	0.075	0.324	0.305	0.176	0.0
MCDR1	(Interval)	98.1										
D6S434	4.3	102.4	$-\varepsilon$	−4.496	−3.103	−2.507	−1.163	−0.632	−0.183	−0.005	0.043	0.0
CORD9	(Interval)	47.6										
D8S1820	0	47.6	$-\varepsilon$	−11.981	−8.501	−7.014	−3.65	−2.277	−1.002	−0.385	−0.092	0.1

ELOVL4. We have reported cloning and characterization of the *ELOVL4* gene in the cynomolgus monkey.[41] Three mutations leading to truncation of the *ELOVL4* protein were reported in humans with Stargardt-like macular dystrophy[23,42] (Karen G, et al. *IOVS* 2004;45:ARVO E-Abstract 1766). Mutation analysis of monkeys with macular degeneration did not detect any amino acid-altering sequence changes. Silent polymorphisms were observed in exons 1, 3, and 4 of the *ELOVL4* gene.

Linkage Analysis of Candidate Gene Loci

The methodology we used to screen for mutations in the candidate genes could miss disease-associated changes that may be present in the promoter or intronic regions; therefore, linkage analysis was performed to exclude the five genes further. Moreover, the macular degeneration phenotype in the monkey pedigree could be caused by a single gene defect. In these cases, linkage analysis would be a comprehensive approach to confirm or exclude a particular gene locus. Microsatellite markers linked to the five candidate gene loci in addition to eight human macular degeneration loci—*ABCA4*, *VMD2*, *DHRD* (*EFEMP1*), *TIMP3*, *STGD3* (*ELOVL4*), Cone rod dystrophy-8 (*CORD-8*), age-related macular degeneration 1 (*ARMD1*, gene Hemicentin1), rhodopsin, *STGD4*, North Carolina macular degeneration (*MCDR1*), *CORD9*, late-onset retinal degeneration (*CTRP5*), and *CORD5* loci—were analyzed to test for linkage with the macular degeneration in the monkey pedigree. None of the tested loci gave significant positive lod scores (Table 4). We also constructed haplotypes using the genotype data of markers at the 13 loci. This analysis further supported the exclusion of these loci from being among those that might harbor the gene associated with macular degeneration in these monkeys.

Discussion

We report a detailed description of early-onset macular degeneration in cynomolgus monkeys and the exclusion of known genes responsible for macular degeneration in humans as a disease-associated gene in this animal model. Several forms of macular degeneration have been described in humans, including autosomal dominant, autosomal recessive, and X-linked modes of inheritance. The most common form of macular disease in humans is AMD. Major clinical characteristics of AMD are loss of central vision with RPE atrophy or exudation. The presence of subretinal deposits known as drusen is one of the early signs observed in AMD and several other macular degenerations. Recent studies suggest that the process of drusen formation includes inflammatory and immune-mediated events.[35] Immunohistochemical examinations have revealed that drusen contains activated complement factors. These molecules include C5, the cleavage product of C3 (C3b, iC3b, and C3dg), and the terminal complement complex C5b-9. Clinical and histologic studies of the affected monkeys showed the presence of drusen (Figs. 2, 3). Immunologic analysis demonstrated that drusen in monkeys had C5 as a component, suggesting that the nature of monkey drusen was similar to that reported in human AMD. At the same time, the onset of the disease in monkeys is at ~2 years of age; therefore, the monkey macular degeneration resembles early-onset human macular degeneration with drusen.

Comparison of the gene maps and chromosome painting data revealed a high degree of synteny and genome conservation between human and Macaque genomes.[43,44] Amplification of cynomolgus monkey DNA with human microsatellite marker primers and sequence analysis revealed that not only the sequences flanking the microsatellite repeat regions but also the polymorphic nature of these repeats is conserved between human and monkey genomes (data not shown). Comparative studies on human and chimpanzee genomes have shown the same average heterozygosity at microsatellite marker loci and conserved genetic distance between markers.[45] Molecular cloning of monkey orthologues of the human *ABCA4*, *VMD2*, *EFEMP1*, *TIMP3*, and *ELOVL4* genes further demonstrated the high conservation between the human and macaque genomes not only in the organization of the gene structure, but also at the sequence level. Considering the high conservation between human and macaque genomes, human macular degeneration loci can be considered plausible candidates for identification of the gene associated with macular degeneration in the monkeys. We tested this hypothesis using microsatellite markers linked to human macular degeneration loci and successfully amplified microsatellites in the monkey DNA with human primers. However, we failed to establish linkage with the tested loci, and the subsequent haplotype analysis further confirmed this finding. Therefore, the macular degeneration locus in the monkey pedigree is not likely to be associated with the regions of the monkey genome that are syntenic to human genomic regions comprising the 13 macular disease loci tested. Mutation analysis of candidate genes also supported the exclusion of the *ABCA4*, *VMD2*, *EFEMP1*, *TIMP3*, and *ELOVL4* genes. The analyses detected five- and six-amino-acid substitutions in the *ABCA4* and *VMD2* genes, respectively. Some silent nucleotide substitutions or intronic sequences changes, such as small insertions/deletions, SNPs, and variations of short tandem repeats were observed in the *EFEMP1*, *TIMP3*, and *ELOVL4* genes. All these sequence variants did not segregate with the disease phenotype in the extended pedigree. Hence, these changes were interpreted as benign polymorphisms.

In the *ABCA4* sequence of a normal monkey, we found two amino acid replacements (K223Q and R1300Q) that are associated with Stargardt disease in humans. Because of the extensive conservation between the monkey and human gene sequences, one would expect these amino acid changes to have similar disease-associated effects in monkeys. One explanation of this discrepancy could be that K223Q and R1300Q are not causing the disease phenotype in humans, but rather represent markers linked to disease-causing mutations somewhere else in the gene. Alternatively, the disease-causing effect of these amino acid changes on the function of the human ABCA4 protein could be eliminated or compensated for by other differences in the monkey protein. Comparative analysis of the monkey and human genes may provide clues for understanding the molecular pathogenesis caused by *ABCA4* variation. In the *VMD2* gene sequence of normal monkeys, we found a nonsense mutation at codon 582. The change is located at the fourth residue from the C terminus. Bestrophin was shown to form oligomeric chloride channels in cell membranes.[37] The C-terminal cytosolic tail, encoded by exons 10 and 11, has been reported not to be essential for the protein's function. Moreover, although 72 nucleotide substitutions have been identified in Best disease to date,[3,7,26] none of them is reported in exons 10 and 11. Hence, the deletion of four amino acids from the C-terminal end of the protein could be considered not to be associated with the disease.

In summary, we demonstrated that none of the 13 human macular degeneration loci tested were involved in causing the macular degeneration phenotype observed in the monkey pedigree. These results demonstrate the need for additional studies to identify the genetic locus associated with the phenotype in these monkeys and to understand the genetic defect underlying the disease. Identification of the gene responsible for this specific macular degeneration phenotype not only defines a new candidate locus for human macular degeneration, but also provides a primate animal model that can be extensively studied for elucidation of the mechanisms, diagnosis, prophylaxis, and treatment of macular degenerations, including AMD.

References

1. Michaelides M, Hunt DM, Moore AT. The genetics of inherited macular dystrophies. *J Med Genet.* 2003;9:641-650.
2. Allikmets R, Singh N, Sun H, et al. A photoreceptor cell-specific ATP-binding transporter gene (ABCR) is mutated in recessive Stargardt macular dystrophy. *Nat Genet.* 1997;3:236-246.
3. Petrukhin K, Koisti MJ, Bakall B, et al. Identification of the gene responsible for Best macular dystrophy. *Nat Genet.* 1998;3:241-247.
4. Stone EM, Lotery AJ, Munier FL, et al. A single EFEMP1 mutation associated with both Malattia Leventinese and Doyne honeycomb retinal dystrophy. *Nat Genet.* 1999;2:199-202.
5. Weber BH, Vogt G, Pruett RC, Stohr H, Felbor U. Mutations in the tissue inhibitor of metalloproteinases-3 (TIMP3) in patients with Sorsby's fundus dystrophy. *Nat Genet.* 1994;4:352-356.
6. Zhang K, Kniazeva M, Han M, et al. A 5-bp deletion in ELOVL4 is associated with two related forms of autosomal dominant macular dystrophy. *Nat Genet.* 2001;1:89-93.
7. Marquardt A, Stohr H, Passmore LA, et al. Mutations in a novel gene, VMD2, encoding a protein of unknown properties cause juvenile-onset vitelliform macular dystrophy (Best's disease). *Hum Mol Genet.* 1998;9:1517-1525.
8. Bernstein PS, Tammur J, Singh N, et al. Diverse macular dystrophy phenotype caused by a novel complex mutation in the *ELOVL4* gene. *Invest Ophthalmol Vis Sci.* 2001;13:3331-3336.
9. Dithmar S, Curcio CA, Le NA, Brown S, Grossniklaus HE. Ultrastructural changes in Bruch's membrane of apolipoprotein E-deficient mice. *Invest Ophthalmol Vis Sci.* 2000;8:2035-2042.
10. Mata NL, Tzekov RT, Liu X, et al. Delayed dark-adaptation and lipofuscin accumulation in abcr+/− mice: implications for involvement of ABCR in age-related macular degeneration. *Invest Ophthalmol Vis Sci.* 2001;8:1685-1690.

11. Rakoczy PE, Zhang D, Robertson T, et al. Progressive age-related changes similar to age-related macular degeneration in a transgenic mouse model. *Am J Pathol.* 2002;4:1515–1524.
12. Stafford TJ. Maculopathy in an elderly sub-human primate. *Mod Probl Ophthalmol.* 1974;0:214–219.
13. El-Mofty A, Gouras P, Eisner G, Balazs EA. Macular degeneration in rhesus monkey (Macaca mulatta). *Exp Eye Res.* 1978;4:499–502.
14. Hope GM, Dawson WW, Engel HM, et al. A primate model for age related macular drusen. *Br J Ophthalmol.* 1992;1:11–16.
15. Nicolas MG, Fujiki K, Murayama K, et al. Studies on the mechanism of early onset macular degeneration in cynomolgus monkeys. II. Suppression of metallothionein synthesis in the retina in oxidative stress. *Exp Eye Res.* 1996;4:399–408.
16. Nicolas MG, Fujiki K, Murayama K, et al. Studies on the mechanism of early onset macular degeneration in cynomolgus (Macaca fascicularis) monkeys. I. Abnormal concentrations of two proteins in the retina. *Exp Eye Res.* 1996;3:211–219.
17. Suzuki MT, Terao K, Yoshikawa Y. Familial early onset macular degeneration in cynomolgus monkeys (Macaca fascicularis). *Primates.* 2003;3:291–294.
18. Klaver CC, Wolfs RC, Assink JJ, et al. Genetic risk of age-related maculopathy: population-based familial aggregation study. *Arch Ophthalmol.* 1998;12:1646–1651.
19. Seddon JM, Ajani UA, Mitchell BD. Familial aggregation of age-related maculopathy. *Am J Ophthalmol.* 1997;2:199–206.
20. Meyers SM, Greene T, Gutman FA. A twin study of age-related macular degeneration. *Am J Ophthalmol.* 1995;6:757–766.
21. Tuo J, Bojanowski CM, Chan CC. Genetic factors of age-related macular degeneration. *Prog Retin Eye Res.* 2004;2:229–249.
22. Abecasis GR, Yashar BM, Zhao Y, et al. Age-related macular degeneration: a high-resolution genome scan for susceptibility loci in a population enriched for late-stage disease. *Am J Hum Genet.* 2004;3:482–494.
23. Ayyagari R, Zhang K, Hutchinson A, et al. Evaluation of the ELOVL4 gene in patients with age-related macular degeneration. *Ophthalmic Genet.* 2001;4:233–239.
24. Allikmets R. Further evidence for an association of ABCR alleles with age-related macular degeneration: the International ABCR Screening Consortium. *Am J Hum Genet.* 2000;2:487–491.
25. Felbor U, Doepner D, Schneider U, Zrenner E, Weber BH. Evaluation of the gene encoding the tissue inhibitor of metalloproteinases-3 in various maculopathies. *Invest Ophthalmol Vis Sci.* 1997; 6:1054–1059.
26. Lotery AJ, Munier FL, Fishman GA, et al. Allelic variation in the VMD2 gene in best disease and age-related macular degeneration. *Invest Ophthalmol Vis Sci.* 2000;6:1291–1296.
27. Honjo S. The Japanese Tsukuba Primate Center for Medical Science (TPC): an outline. *J Med Primatol.* 1985;2:75–89.
28. Marmor MF, Zrenner E. Standard for clinical electroretinography (1999 update): International Society for Clinical Electrophysiology of Vision. *Doc Ophthalmol.* 1998;2:143–156.
29. Dockhorn-Dworniczak B, Dworniczak B, Brommelkamp L, et al. Non-isotopic detection of single strand conformation polymorphism (PCR-SSCP): a rapid and sensitive technique in diagnosis of phenylketonuria. *Nucleic Acids Res.* 1991;9:2500.
30. Liu W, Smith DI, Rechtzigel KJ, Thibodeau SN, James CD. Denaturing high performance liquid chromatography (DHPLC) used in the detection of germline and somatic mutations. *Nucleic Acids Res.* 1998;6:1396–1400.
31. Griesinger IB, Sieving PA, Ayyagari R. Autosomal dominant macular atrophy at 6q14 excludes CORD7 and MCDR1/PBCRA loci. *Invest Ophthalmol Vis Sci.* 2000;1:248–255.
32. Terwilliger JD, Ott J. *Handbook of Human Genetic Linkage.* Baltimore, MD: The Johns Hopkins University Press; 1994.
33. Otto J. *Analysis of Human Genetic Linkage.* Baltimore, MD: The Johns Hopkins University Press; 1999.
34. Khani SC, Karoukis AJ, Young JE, et al. Late-onset autosomal dominant macular dystrophy with choroidal neovascularization and nonexudative maculopathy associated with mutation in the RDS gene. *Invest Ophthalmol Vis Sci.* 2003;8:3570–3577.
35. Mullins RF, Russell SR, Anderson DH, and Hageman GS. Drusen associated with aging and age-related macular degeneration contain proteins common to extracellular deposits associated with atherosclerosis, elastosis, amyloidosis, and dense deposit disease. *FASEB J.* 2000;7:835–846.
36. Marmorstein AD, Marmorstein LY, Rayborn M, et al. Bestrophin, the product of the Best vitelliform macular dystrophy gene (VMD2), localizes to the basolateral plasma membrane of the retinal pigment epithelium. *Proc Natl Acad Sci USA.* 2000;23: 12758–12763.
37. Sun H, Tsunenari T, Yau KW, Nathans J. The vitelliform macular dystrophy protein defines a new family of chloride channels. *Proc Natl Acad Sci USA.* 2002;6:4008–4013.
38. Tabata Y, Isashiki Y, Kamimura K, Nakao K, Ohba N. A novel splice site mutation in the tissue inhibitor of the metalloproteinases-3 gene in Sorsby's fundus dystrophy with unusual clinical features. *Hum Genet.* 1998;2:179–182.
39. Langton KP, McKie N, Curtis A, et al. A novel tissue inhibitor of metalloproteinases-3 mutation reveals a common molecular phenotype in Sorsby's fundus dystrophy. *J Biol Chem.* 2000;35: 27027–27031.
40. Felbor U, Stohr H, Amann T, Schonherr U, Weber BH. A novel Ser156Cys mutation in the tissue inhibitor of metalloproteinases-3 (TIMP3) in Sorsby's fundus dystrophy with unusual clinical features. *Hum Mol Genet.* 1995;12:2415–2416.
41. Umeda S, Ayyagari R, Suzuki MT, et al. Molecular cloning of ELOVL4 gene from cynomolgus monkey (Macaca fascicularis). *Exp Anim.* 2003;2:129–135.
42. Edwards AO, Donoso LA, Ritter R III. A novel gene for autosomal dominant Stargardt-like macular dystrophy with homology to the SUR4 protein family. *Invest Ophthalmol Vis Sci.* 2001;11:2652–2663.
43. Wienberg J, Stanyon R. Comparative painting of mammalian chromosomes. *Curr Opin Genet Dev.* 1997;6:784–791.
44. O'Brien SJ, Menotti-Raymond M, Murphy WJ, et al. The promise of comparative genomics in mammals. *Science.* 1999;5439:458–462,479–481.
45. Crouau-Roy B, Service S, Slatkin M, Freimer N. A fine-scale comparison of the human and chimpanzee genomes: linkage, linkage disequilibrium and sequence analysis. *Hum Mol Genet.* 1996;8: 1131–1137.

The FASEB Journal express article 10.1096/fj.04-3525fje. Published online August 26, 2005.

Molecular composition of drusen and possible involvement of anti-retinal autoimmunity in two different forms of macular degeneration in cynomolgus monkey (*Macaca fascicularis*)

Shinsuke Umeda,*,† Michihiro T. Suzuki,‡ Haru Okamoto,* Fumiko Ono,‡ Atsushi Mizota,§ Keiji Terao,‖ Yasuhiro Yoshikawa,† Yasuhiko Tanaka,* and Takeshi Iwata*

*National Institute of Sensory Organs, National Hospital Organization, Tokyo Medical Center, Tokyo 152-8902; †Department of Biomedical Science, Graduate School of Agricultural and Life Sciences, The University of Tokyo, Tokyo 113-8657; ‡The Corporation for Production and Research of Laboratory Primates, Ibaraki 305-0843; §Department of Ophthalmology, Juntendo University Urayasu Hospital, Chiba 279-0021; and ‖Tsukuba Primate Research Center, National Institute of Biomedical Innovation, Ibaraki 305-0843, Japan

Corresponding author: Takeshi Iwata, Ph.D., National Institute of Sensory Organs, National Hospital Organization, Tokyo Medical Center, 2-5-1 Higashigaoka, Meguro-ku, Tokyo 152-8902 Japan. E-mail: iwatatakeshi@kankakuki.go.jp

ABSTRACT

We have previously reported a cynomolgus monkey (*Macaca fascicularis*) pedigree with early onset macular degeneration that develops drusen at 2 yr after birth (1). In this study, the molecular composition of drusen in monkeys affected with late onset and early onset macular degeneration was both characterized. Involvement of anti-retinalautoimmunity in the deposition of drusen and the pathogenesis of the disease was also evaluated. Funduscopic and histological examinations were performed on 278 adult monkeys (mean age=16.94 yr) for late onset macular degeneration. The molecular composition of drusen was analyzed by immunohistochemistry and/or direct proteome analysis using liquid chromatography tandem mass spectroscopy (LC-MS/MS). Anti-retinal autoantibodies in sera were screened in 20 affected and 10 age-matched control monkeys by Western blot techniques. Immunogenic molecules were identified by 2D electrophoresis and LC-MS/MS. Relative antibody titer against each antigen was determined by ELISA in sera from 42 affected (late onset) and 41 normal monkeys. Yellowish-white spots in the macular region were observed in 90 (32%) of the late onset monkeys that were examined. Histological examination demonstrated that drusen or degenerative retinal pigment epithelium (RPE) cells were associated with the pigmentary abnormalities. Drusen in both late and early onset monkeys showed immunoreactivities for apolipoprotein E, amyloid P component, complement component C5, the terminal C5b-9 complement complex, vitronectin, and membrane cofactor protein. LC-MS/MS analyses identified 60 proteins as constituents of drusen, including a number of common components in drusen of human age-related macular degeneration (AMD), such as annexins, crystallins, immunoglobulins, and complement

components. Half of the affected monkeys had single or multiple autoantibodies against 38, 40, 50, and 60 kDa retinal proteins. The reacting antigens of 38 and 40 kDa were identified as annexin II and μ-crystallin, respectively. Relative antibody titer against annexin II in affected monkeys was significantly higher than control animals ($P<0.01$). Significant difference was not observed in antibody titer against μ-crystallin; however, several affected monkeys showed considerably elevated titer (360–610%) compared with the mean for unaffected animals. Monkey drusen both in late and early onset forms of macular degeneration had common components with drusen in human AMD patients, indicating that chronic inflammation mediated by complement activation might also be involved in the formation of drusen in these affected monkeys. The high prevalence of anti-retinalautoantibodies in sera from affected monkeys demonstrated an autoimmune aspect of the pathogenesis of the disease. Although further analyses are required to determine whether and how autoantibodies against annexin II or μ-crystallin relate to the pathogenesis of the disease, it could be hypothesized that immune responses directed against these antigens might trigger chronic activation of the complement cascade at the site of drusen formation.

Key words: liquid chromatography tandem mass spectroscopy

Age-related macular degeneration (AMD) is the most common cause of legal blindness in people over 60 yr of age and is estimated to affect millions of individuals in industrialized countries. Among people over 75 yr of age, mild or early forms occur in nearly 30% and the advanced form in ~7% of the population (2). Taking high levels of antioxidants and zinc are shown to reduce the risk of developing advanced form by the Age-Related Eye Disease Study (AREDS) (3). The AREDS formulation, while not a cure for AMD, may play a key role in helping people at high risk for developing advanced AMD keep their remaining vision. At present there is no fundamental cure for AMD, although some success in attenuating choroidal neovascularization has been obtained with surgical excision or photodynamic therapy.

Major clinical characteristics of AMD are loss of central vision with choroidal neovascularization and geographic atrophy, where atrophy occurs around the choriocapillaris with clear boundaries. The accumulation of debris-like material between the retinal pigment epithelium (RPE) and Bruch's membrane is observed to precede this exudation and atrophy. Although the most prominent lesion of AMD involves the RPE and Bruch's membrane, it is degeneration, dysfunction, and death of photoreceptors and its consequences that account for the vision loss. Very little is known about the pathophysiology of this disease process. The debris-like material, referred to as drusen, is regarded as a hallmark risk factor for developing AMD. The presence of numerous and/or confluent drusen in the macula is widely accepted as a sign of the early stage of AMD, whereas their composition and mechanism of formation remains controversial.

Drusen or drusen-like bodies have been reported in macaque monkeys since the 1970s (4). Aged monkeys spontaneously show macular degenerative changes, such as pigment mottling, hyper- or hypopigmentation, and drusen in the macula (5, 6). The late onset form of macular degeneration in these monkeys is consistent with the phenotype observed in the early stage of AMD. Thus, macaque monkeys have been suggested as an optimum animal model for AMD (7, 8). In addition, we have previously reported an early onset macular degeneration in a cynomolgus monkey pedigree maintained at Tsukuba Primate Center (9–11). For these monkeys,

the symptoms appear early in life around the age of 2 yr and progress slowly throughout life. The disease has been shown to have autosomal dominant inheritance (12). These two forms of macular degeneration, late onset and early onset, in monkeys could be extremely valuable models of the early stage of AMD, especially for elucidating the mechanism of drusen formation. However, the molecular properties of drusen observed in monkeys have not been described to date. Comparative studies of the molecular composition of drusen in monkeys and humans are required to establish these macular degeneration monkeys as AMD models.

Drusen composition and origin have been analyzed extensively in AMD. Various lipids, polysaccarides, and glycosaminoglycans have been identified as constituents (13). Recent immunohistochemical studies have revealed that drusen contains protein molecules that mediate inflammatory and immune processes (14, 15). These components include immunoglobulins, components of the complement pathway, modulators of complement activation (e.g., vitronectin, clusterin, membrane cofactor protein, and complement receptor 1), molecules involved in the acute-phase response to inflammation (e.g., amyloid P component, α1-antitrypsin, and apolipoprotein E), major histocompatibility complex class II antigens, and HLA-DR antigens. Cellular components have also been identified in drusen, including RPE debris, lipofuscin, and melanin. These findings have led to the suggestion that immune complex-mediated inflammation damages RPE cells, while RPE cells respond by secreting proteins that modulate the immune response. Shedding or endocytosis of cell membranes of injured RPE is postulated to function as the core for these secreted components to accumulate and form extracellular deposits (13).

Furthermore, the codistribution of IgG and terminal complement complexes in drusen suggests an immune response directed against retinal antigens and immune complex formation (16). This hypothesis is supported by the presence of putative anti-retinalautoantibodies in the sera of patients with AMD (17, 18). Anti-retinalautoantibodies have previously been reported in a number of retinal diseases, including retinitis pigmentosa (19), paraneoplastic retinopathies (20), and retinal vasculitis (21). In addition, patients with membranoproliferative glomerulonephritis who suffer from glomerular injury caused by complement activation and immune complex deposition are known to develop drusen resembling those of AMD by ultrastructure and composition (22). To date, the role of anti-retinal autoantibodies in the pathogenesis of AMD has not been fully examined. It remains unknown whether the initiation of chronic inflammation and subsequent drusen formation require autoimmune-mediated events as a primary initiating factor. To clarify the role of autoimmunity in AMD, the antigens eliciting circulating anti-retinal autoantibodies need to be identified.

In this study, the molecular composition of drusen observed in late onset and early onset macular degeneration monkeys was investigated by immunohistochemistry and proteome analysis for comparison with drusen in AMD. Involvement of anti-retinalautoimmunity in late onset monkeys was subsequently examined. Anti-retinalautoantibodies in sera from affected monkeys were screened, and the immunogenic molecules eliciting these autoantibodies were determined by LC-MS/MS. Relative levels of autoantibodies against the identified antigens were determined in sera from affected and unaffected monkeys. Better understanding of the molecules involved in drusen composition and autoimmunity will improve evaluation of the macular degeneration monkeys as human AMD models. Furthermore, this information should also provide important clues to aid in the development of possible therapeutic reagents for prevention of drusen formation.

MATERIALS AND METHODS

Maintenance of monkeys

The cynomolgus monkey pedigree with early onset macular degeneration was reared in Tsukuba Primate Research Center, National Institute of Biomedical Innovation. All monkeys were treated in accordance with the rules for care and management of the Tsukuba Primate Center (11) under the Guiding Principles for Animal Experiments using Non-Human Primates formulated and enforced by the Primate Society of Japan (Primate Society of Japan, 1986). All experimental procedures were approved by the Animal Welfare and Animal Care Committee of the National Institute of Biomedical Innovation. The monkeys used for studies of late onset macular degeneration were reared in large-scale breeding facilities in Manila, Philippines (Simian Conservation Breeding and Research Center, Inc.,). The facilities are accredited by the Association for Assessment and Accreditation of Laboratory Animal Care International (AAALAC International). Monkeys were routinely examined for physical and ophthalmic conditions by veterinarians and by ophthalmologists, respectively.

Clinical studies

At the breeding facility of the Simian Conservation Breeding and Research Center, 278 female monkeys ranging from 13 to 25 yr old were examined. The mean age was 16.94 yr old, and the median age was 17 yr. The clinical examination was performed after tranquilization by intramuscular injection of 10 mg/kg ketamine-HCl (Ketalar-50; Sankyo, Tokyo). Approximately 20 min before examination of the ocular fundi, one drop of a mixture of 0.5% tropicamide and 0.5% phenylephrine hydrochloride (Mydrin-P; Santen Pharmaceutical, Oosaka, Japan) was instilled into each eye of each animal for dilation of the pupils. The cornea was kept moist with artificial tears. Fundus examination and fluorescein angiography (FA) were performed using a TRC50 fundus camera (Topcon, Tokyo, Japan). For FA, 0.5 ml of 1% fluorescein solution (Fluorescite; Alcon Japan, Tokyo, Japan) was intravenously injected.

Immunohistochemical studies of drusen components

Enucleated eyes were fixed in 10% neutralized and buffered formaldehyde solution at 4°C overnight and then dehydrated. The specimens were embedded in paraffin and sectioned to prepare serial sections of 4 μm thicknesses. The specimens were treated for antigen retrieval with 0.4 mg/ml proteinase K in phosphate buffered saline (PBS) for 5 min at room temperature or by autoclaving in Target Retrieval Solution (Dako, Carpinteria, CA) for 20 min at 121°C. Subsequently, the sections were blocked with 5% skim milk in PBS. The specimens were then reacted with primary antibodies diluted in PBS for 2 h at room temperature. Conditions for antigen retrieval and dilution of primary antibodies for each antigen are shown in Table 1. After being washed, the sections were incubated with Alexa 488 conjugated goat anti-rabbit or mouse IgG (Molecular Probes, Eugene, OR) diluted 1:200 in PBS for fluorescent signal detection. The negative control stainings were performed with normal rabbit or mouse immunoglobulin fraction (Dako) instead of primary antibodies. After being processed, sections were examined using a confocal laser scanning microscope (Radiance 2100, Bio-Rad, Richmond, CA). Images were acquired with Lasersharp software. Double-labeled images were generated by the green channel for each antigen and red channel for autofluorescence emitted by lipofuscin pigment in the RPE.

Drusen isolation

After an eyeball was thawed on ice, the anterior segment was removed with a circumferential cut behind the limbus. The optic nerve was cut, and the posterior pole was laid open with longitudinal incisions leaving the macular region intact. The vitreous and neural retina were removed under a stereoscopic microscope (SMZ800, Nikon, Tokyo, Japan). The RPE was washed away from the interior surface of the globe with 100 mM ammonium bicarbonate buffer (pH 8.0). At magnifications between 20 and 30 diameters, drusen were scraped up with a tiny tungsten needle, the needlepoint of which was 1 μm diameter (ST Japan, Tokyo, Japan), and transferred to ammonium bicarbonate buffer in tubes. Smaller drusen was collected by aspiration in the presence of the same buffer with a micro pipette (PrimeTech, Ibaraki, Japan) and a microinjector pump (Narishige, Tokyo, Japan). Isolated drusen were stored at -80°C until further analyses.

Direct proteome analysis of drusen components

Ten micrograms of isolated drusen suspended in ammonium bicarbonate buffer were dried and redissolved in 20 μl of the same buffer. Cysteine was reduced by adding 20 μl of 50 mM DTT and incubating for 1 h at 37°C. Subsequently, 20 μl of 100 mM iodoacetamide were added and the alkylation continued 30 min at room temperature in the dark. The preparation was then digested with 1 μg of trypsin at 37°C overnight. The resultant tryptic peptides were dried, resuspended in 40 μl of aqueous 0.1% trifluoroacetic acid/10% acetonitrile, and analyzed by LC-MS/MS with a Paradigm system (Michrom Bioresources, Auburn, CA) and an ion trap mass spectrometer (LCQ DECA XP; Thermo Electron, Kanagawa, Japan). Peptides were separated on a Magic C18 column (200 μm ID×5 cm, particle size 5 μm, pore size 200 Å; Michrom Bioresources) by using aqueous formic acid/acetonitrile solvents, a flow rate of 3 μl/min, and a gradient of 5–65% acetonitrile over 120 min. Protein identification from MS/MS spectra was performed using protein identification software (Bioworks 3.0, Thermo Electron) and National Center for Biotechnology Information protein sequence databases.

Screening for anti-retinal autoantibodies in affected monkey sera

The neural retina and choroid isolated from unaffected monkeys (4 yr old) were homogenized in lysis buffer containing 50 mM Tris-HCl (pH 7.5), 2 mM EDTA, 0.5% TritonX-100, 2% SDS, and protease inhibitors (Complete; Roche, Mammheim, Germany). After centrifugation at 16,000 *g* for 30 min at 4°C, the supernatant was collected. Fifteen micrograms of the extracted retinal proteins were mixed with sample buffer (Laemmli sample buffer; Bio-Rad), boiled for 3 min, and separated on 12.5% gel by SDS-PAGE. After transfer to PVDF membranes, the blots were cut into strips by single lane width. The individual strip was blocked with 5% skim milk in PBS containing 0.05% Tween 20 and then reacted with serum from an affected or unaffected monkey diluted (1:1000) in 2% BSA-PBS-0.1% Tween. Sera collected from 20 affected and 10 age-matched control monkeys were used. After incubation for 1 h at room temperature, the strips were washed four times with PBS-0.2% Tween and reacted with peroxidase-conjugated rabbit anti-human Ig (A+G+M) antibodies (Jackson ImmunoResearch Laboratories, West Grove, PA) diluted (1:50,000) with 5% skim milk-PBS-0.1% Tween for 30 min at room temperature. After five washes, the strips were incubated with chemiluminescent substrate (SuperSignal West Femto Maximum Sensitivity Substrate; Pierce, Rockford, IL). The resultant signals were detected and captured with Lumi-Imager F1 (Roche).

Identification of retinal autoantigens

Proteins were extracted from neural retina and choroid isolated from unaffected monkeys. Subsequently, the total protein solution was precipitated by changing solvent composition in a step-wise fashion such that a set of seven protein fractions was produced. These procedures were carried out using 2-D Fractionation kit (Amersham Biosciences, Buckinghamshire, UK). Eight micrograms of protein from each fraction were separated by SDS-PAGE, transferred to PVDF membranes, and immunoblotted with sera as described above. The protein fraction that reacted most intensively was dialyzed against 7 M urea/2 M thiourea at 4°C overnight. To the dialyzed protein solution was then added 4× sample buffer containing 200 mM DTT, 16% CHAPS, 0.8% carrier ampholytes. The samples were separated by 2-D electrophoresis. One hundred micrograms protein were loaded on immobilized pH gradient (IPG) strips (pH 3–10, 4–7, 7 cm; Bio-Rad) by in-gel rehydration at 20°C overnight. For the first dimension, isoelectric focusing (IEF) was performed with initial voltage 250 V for 15 min and then increased to 4,000 V for 1 h and held until 20,000 Vhr was reached. Immediately after IEF, the IPG strips were equilibrated for 20 min in buffer containing 6 M urea, 2% SDS, 0.375 M Tris (pH 8.8), and 20% glycerol under reducing conditions with 2% DTT, followed by another incubation for 10 min in the same buffer under alkylating conditions with 2.5% iodoacetamide. Equilibrated IPG strips were then electophoresed for the second-dimension by SDS-PAGE. After transfer to PVDF membranes, immunoblotting with sera was performed as described above. The image of chemiluminescent signals was captured and merged with that of protein spots visualized by SYPRO Ruby (Bio-Rad), and the spots corresponding to the immunoreactivity were excised. The excised gel pieces were washed with 100 mM ammonium bicarbonate and then with acetonitrile. After the washing steps, gel pieces were completely dried for the reduction-alkylation step. The supernatant was removed, and the washing procedure was repeated three times. Finally, gel pieces were again completely dried before tryptic digestion and swelled in a solution of trypsin (12.5 ng/μl; Promega, Madison, WI) in 50 mM ammonium bicarbonate. The digestion was performed for 16 h at 37°C, and the extraction step was performed with 5% formic acid in 50% acetonitrile. The extracted peptides were pooled and dried. After being resuspended in 40 μl of aqueous 0.1% trifluoroacetic acid/10% acetonitrile, the samples were analyzed by LC-MS/MS as described above.

Expression and purification of recombinant proteins

The open reading frames of human annexin II and μ-crystallin were amplified by PCR from cDNA mixture synthesized from kidney, brain, liver, placenta, and lung (5′-RACE Ready cDNA; Clontech, Palo Alto, CA). Sense primer 5′-ATGTCTACTGTTCACGAAATCCTG-3′ and antisense primer 5′-TCAGTCATCTCCACCACACAG for annexin II, and sense primer 5′-ATGAGCCGGGTACCAGC-3′ and antisense primer 5′-TTATTTACCAGATGACCAGGAATC-3′ for μ-crystallin were used for amplification. The amplified products were subcloned into plasmid vectors (pTrc-His A; Invitrogen, Carlsbad, CA) with an N-terminal 6×His tag. The construct was transformed into *E. coli* (TOP10 cells; Invitrogen), and expression was induced with isopropyl-β-thiogalactoside. Bacteria were then lysed in buffer containing 8 M urea, 0.5 M NaCl, and 20 mM sodium phosphate (pH 7.4). Recombinant proteins were purified using affinity columns charged with Ni^{2+} ions (HiTrap Chelating HP; Amersham Biosciences), with a final elution using the same buffer with lowered pH (3.5).

ELISA for autoantibody titer

The purified recombinant protein was diluted (0.5 μg/ml) with sodium bicarbonate buffer (pH 9.6), and immobilized in 96-well immunoplates (Nalge Nunc, Rochester, NY). After being washed with 0.05% Tween 20 in PBS, the sample wells were blocked with sodium bicarbonate buffer containing 3% BSA for 2 h at room temperature. The sample wells were washed before the addition of sera diluted (1:50) with 1% BSA-PBS-Tween 0.05%. Sera collected from 42 affected and 41 age-matched control monkeys were used. After incubation for 2 h at room temperature, the plates were washed and reacted with peroxidase-conjugated rabbit anti-human Ig(A+G+M) antibodies (Jackson ImmunoResearch Laboratories) diluted (1:50,000) with 1% BSA-PBS-Tween 0.05% for 30 min at room temperature. After the final wash, 3,3′,5,5′-tetramethylbenzidine substrate (Bio-Rad) was added to each well and incubated for color development. The reaction was stopped by adding 1 N HCl, and the absorbance at 450 nm was read.

Expression of annexin II in the retina

Protein extracts were prepared separately from the whole retina, neurosensory retina, and choroid including the RPE, which were isolated from unaffected monkeys, and also from cultured human primary RPE cells. The samples were applied to SDS-PAGE, transferred to membrane, and then immunoreacted with mouse anti-annexin II monoclonal antibody (Zymed Laboratories, South San Francisco, CA). Protein extract from Madin-Darby canine kidney (MDCK) cells, which are known to express annexin II abundantly, was used for positive control.

RESULTS

Clinical and histological findings of late onset macular degeneration monkeys

The fundus oculi of 278 aged monkeys (mean age: 16.94 yr) were funduscopically examined 3 times from 2001 to 2004. The fundus appearance typical of a monkey with late onset macular degeneration is shown in Fig. 1*A*. Fine yellowish-white dots are observed in the macula. In the most cases, the locations of the lesions fell within the region centered on the fovea centralis within a diameter equal to one optic disc. These pigmentary abnormalities could be observed in 32% of the population. Of the 278 animals, 67.6% had normal macula with no detectable pigmentary abnormalities, 10.8% were diagnosed as a mild grade with fewer than 5 yellowish-white spots, 11.2% as a moderate grade with 5 to 20 spots, and 10.4% as a severe grade with more than 20 spots (Table 2). The most severe 12 cases were further examined by FA. FA of the same monkey is shown in Fig. 1*B*. Hyperfluorescein dots could be observed corresponding to the spots in fundus photograph. Neither choroidal neovascularization nor disciform scarring was observed in any of the animals examined. No abnormalities were found in the optic disc or blood vessels. Histological studies were performed on 23 monkeys diagnosed as severe, including the 12 animals examined by FA. Drusen in the foveal or parafoveal region could be detected in eight monkeys unilaterally. The fundus and FA photographs of a typical monkey retina with drusen are shown in Fig. 1*C* and *D*). Hyperfluorescent dots had the same distribution as yellowish-white spots in the fundus photograph. In these eyes, various sized drusen accumulated between the RPE and choriocapillaris in the macular region (Fig. 1*E*). Drusen that had an eosinophilic inclusion could be observed (indicated by an asterisk in Fig. 1*F*). This spherical structure could be considered to originate from injured RPE cells, because it showed equivalent

autofluorescence to that emitted by lipofuscin granules in the RPE cells (Fig. 1*G*). Photoreceptor inner and outer segments appeared largely normal. In 15 of the 23 monkeys for which the eyes were examined histologically, including the monkey shown in Fig. 1*A* and *B*, drusen were not observed, but vacuolation and hyper- or hypopigmentation of the RPE cells could be observed corresponding to the yellowish-white spots in the fundus photographs (indicated by arrows in Fig. 1*H*). The vacuolated cells could be considered as aging, lipid-laden RPE cells.

Immunohistochemical and direct proteome analysis of monkey drusen

The protein components of drusen in monkeys were investigated by immunohistochemical methods. In addition to the eight monkeys affected with the late onset macular degeneration, which were histologically confirmed to have drusen, two affected monkeys from the pedigree with early onset macular degeneration were examined. Clinical and histological findings for drusen in early onset macular degeneration were described previously (1). Serial sections of the affected retinas with drusen were incubated with antibodies directed against proteins known to be present in drusen in AMD (14) (Table 1). All drusen in both late onset and early onset macular degeneration were heterogeneously bound by antibodies directed against apolipoprotein E (Fig. 2*A* and *B*), amyloid P component (Fig. 2*C* and *D*), complement component C5 (Fig. 2*E* and *F*), the terminal C5b-9 complement complex (Fig. 2*G* and *H*), and fluid phase inhibitor of complement cascade, vitronectin (Fig. 2*I* and *J*). The membrane-associated inhibitor of complement activation, membrane cofactor protein, was localized in membranous forms along the boundaries between drusen and RPE (Fig. 2*K* and *L*). These results indicated that chronic inflammation mediated by complement activation is also involved in the formation of drusen in monkey macular degeneration.

Subsequently, the molecular composition of drusen was further analyzed by direct proteome analysis using mass spectrometry. Drusen were isolated from the contralateral eyes of the four monkeys that were histologically confirmed to have drusen. The FA photograph of a monkey retina used in this experiment is shown in Fig. 3*A*. A number of drusen showing hyperfluorescence could be observed in the parafoveal region (indicated by a rectangle). After the posterior globe was laid open and the vitreous, neural retina, and RPE removed, drusen could be observed attached to the surface of Bruch's membrane at magnifications between 20 and 30 diameters under a stereoscopic microscope (Fig. 3*B*, white materials in a circle). Drusen were isolated with a tiny needle or a micropipette and transferred into ammonium bicarbonate buffer (Fig. 3*C*, arrows). The obtained protein yield was between 10 and 20 μg per preparation. The isolated drusen (10 μg) were digested with trypsin and analyzed by LC-MS/MS. As a result, we identified 60 proteins from three separate preparations and analyses (Table 3). Twenty of the identified proteins had been previously found to be components of drusen in AMD (indicated by bold letters in Table 3) (23). These proteins included annexin V, clusterin, crystallins, and immunoglobulins, in addition to the components identified by immunohistochemical studies, such as apolipoprotein E, complement components, and vitronectin. Additionally, seven proteins represented superfamilies in which other family members were known constituents of drusen in AMD, such as collagens, hemoglobins, histones, immunoglobulins, and tubulins (indicated by italic letters in Table 3). Therefore, one-half of the identified proteins in monkey drusen were identical to, or related to, known components of drusen from human AMD.

Autoimmunity against retinal proteins in late onset monkeys

The evidence of chronic complement activation at the site of drusen formation suggested that immune complex formation might be taking place via an immune response directed against retinal antigens. To evaluate the involvement of anti-retinal autoimmunity, sera from monkeys affected with late onset macular degeneration were immunoreacted with membrane blots of retinal proteins separated by SDS-PAGE. Sera collected from 20 affected animals and 10 age-matched control monkeys were used. Half of the sera from affected monkeys showed single or doublet reacting bands against 38, 40, 50, and 60 kDa proteins by Western blotting. Sera from the other affected monkeys, as well as the 10 unaffected animals, showed little or no reaction. To identify these four antigens, immunoblotting combined with 2-D electrophoresis was performed. After retinal protein extract was fractionated by stepwise precipitations, the fraction containing the highest concentration of the antigens of interest was selected by Western blotting. Subsequently, the selected fraction was separated on 2-D electrophoresis. An image of protein spots visualized by SYPRO Ruby is shown in Fig. 4*A*. After transfer to PVDF membranes, the blot was reacted with sera containing autoantibodies. An image of chemiluminescent signals obtained by immunoreaction with the serum from the same monkey in Fig. 1*C* is shown in Fig. 4*B*. Three immunoreactive spots were detected in a row at approximate size of 38 kDa. The images of protein spots and chemiluminescent signals were merged, and the corresponding protein spots were excised (indicated by circles in Fig. 4*A*). The excised protein spots were subjected to in-gel digestion with trypsin and were analyzed by LC-MS/MS. As a result, the proteins were identified as annexin II. Chemiluminescent signals obtained by immunoreaction with anti-annexin II monoclonal antibodies completely matched with those with the serum (Fig. 4*C*). By the same procedure, the 40 kDa antigen was found to be μ-crystallin, but the 50 and 60 kDa proteins could not be identified.

Evaluation of autoantibody by ELISA using recombinant antigens

Relative antibody titers against annexin II or μ-crystallin in sera collected from 42 affected monkeys with late onset macular degeneration and 41 age-matched control animals were determined by ELISA. The purified recombinant annexin II could be observed on SDS-PAGE gel at ~41 kDa (Fig. 4*D*, lane 1). The recombinant proteins were confirmed to react both with anti-annexin II monoclonal antibodies (lane 2) and with autoantibodies in the sera (lane 3). Immunoreactivity against μ-crystallin was also confirmed by the same procedure (data not shown). These recombinant proteins were immobilized in 96-well plates for ELISA. Relative antibody titer against annexin II in affected monkeys was significantly higher than in control animals ($P<0.01$; Fig. 4*E*). Seven affected monkeys showed more than twice the mean titer of the control group. On the other hand, relative antibody titer against μ-crystallin did not show significant difference between affected and unaffected monkeys. However, several affected monkeys showed considerably elevated titer (360–610%; Fig. 4*F*).

Expression of annexin II in monkey retina

The localization of annexin II in the retina was determined by Western blotting. Annexin II was present in protein extract from whole retina or choroid, but was most abundant in cultured human RPE cells (Fig. 5*A*). The result indicates that annexin II is highly expressed in the RPE cells both in vivo and in vitro. Immunohistochemical analyses failed to detect annexin II in the retinal cross sections but demonstrated remarkable expression in cultured RPE cells (Fig. 5*B*).

DISCUSSION

AMD is the leading cause of blindness in individuals over the age of 60 in industrialized countries. Limited access to human retinal tissues and the lack of good animal models in species with a well-developed macula make this disease difficult to study. Previous attempts to simulate AMD in experimental animals such as rodents through high-fat diets and phototoxicity (24, 25), senescence acceleration (26), or candidate gene manipulation (27–29) have not fully replicated the clinical and histological features of the disease. On the other hand, Macaque monkeys have been known to develop macular degenerative changes with age, including pigment mottling, hyperpigmentation, or hypopigmentation with drusen, consistent with the phenotype observed in the early stage of AMD (4–8). We have recently reported a monkey pedigree with early onset macular degeneration where drusen are observed <2 yr after birth (1). A well-developed macula is found only in primates and birds, thus making a primate model of particular value in elucidating the etiology and the mechanism underlying the disease. Such a value would also be an important bioresource to test new diagnostic techniques and potential therapeutic strategies for the prevention of this disease. However, previous characterization of monkey macular degeneration has not extended beyond clinical and histological studies. Here, we compare the molecular composition of drusen from monkeys with late onset and early onset macular degeneration with human drusen. The investigation extended the hypothesis of the involvement of anti-retinal autoimmunity in the etiology of AMD by identification of an autoantigen expressed in RPE cells.

The study was initiated from clinical observation of late onset macular degeneration in cynomolgus monkeys. A total of 278 aged animals were examined, and 32% of the population showed drusen-like spots in the macular region (Table 2). These affected monkeys were further classified into two clinical entities by histological studies. One was characterized by the formation of drusen (Fig. 1*C–E*) and the other by degenerative changes in RPE cells such as hyperpigmentation, hypopigmentation, and vacuolation (Fig. 1*A*, *B*, and *H*). These vacuolated lipid-laden RPE cells were observed as pigmentary abnormalities in fundus photographs, and window defects by these cells led to drusen-like hyperfluorescence in FA, making true drusen and lipid-laden RPE cells indistinguishable. However, the lipid-laden RPE cells were mostly individual solitary cells and not likely to represent the larger bodies such as those in Fig. 1*C* and *D*. This type resembles the "non-geographic atrophy" reported in the Chesapeake Bay Waterman Study (30) or the "pigmentary abnormality" of the International Classification and Grading System for Age-related Maculopathy and Age-related Macular Degeneration (31). In none of the affected monkeys examined have we observed choroidal neovascularization, disciform scarring, geographic atrophy, or other advanced pathological changes characteristic of later stage AMD. We have concluded the diagnostic of late onset macular degeneration monkeys as macular degeneration by drusen formation or RPE atrophy leading to the abnormal fundus appearances with pigmentary changes. Further examinations are required to determine the prevalence of drusen by histology in late onset macular degeneration monkeys.

Proteome analyses and immunohistochemical study of drusen composition demonstrated that monkey drusen had a number of protein components in common with drusen in human AMD (Fig. 2; Table 3) (23), including annexins, crystallins, immunoglobulins, apolipoprotein E, complement components, clusterin, and vitronectin. Similarities in the molecular composition of drusen suggested chronic inflammation mediated by complement activation driving drusen biogenesis as a common mechanism for both late onset and early onset macular degeneration in